FERMILAB-CONF-10-443-T

PROCEEDINGS OF SCIENCE

Leptophilic Dark Matter in Direct Detection Experiments and in the Sun

Joachim KOPP*
Fermilab, PO Box 500, Batavia, IL 60510, USA
E-mail: jkopp@fnal.gov

Viviana NIRO
Max-Planck-Institute for Nuclear Physics, PO Box 103980, 69029 Heidelberg, Germany
E-mail: niro@mpi-hd.mpg.de

Thomas SCHWETZ
Max-Planck-Institute for Nuclear Physics, PO Box 103980, 69029 Heidelberg, Germany
E-mail: schwetz@mpi-hd.mpg.de

Jure ZUPAN
Faculty of Mathematics and Physics, Univ. of Ljubljana, Jadranska 19, 1000 Ljubljana, Slovenia
Department of Physics, University of Cincinnati, Cincinnati, Ohio 45221, USA
Josef Stefan Institute, Jamova 39, 1000 Ljubljana, Slovenia
SISSA, Via Bonomea 265, I 34136 Trieste, Italy
E-mail: jure.zupan@cern.ch

Dark matter interacting predominantly with leptons instead of nuclear matter has received a lot of interest recently. In this talk, we investigate the signals expected from such 'leptophilic Dark Matter' in direct detection experiments and in experiments looking for Dark Matter annihilation into neutrinos in the Sun. In a model-independent framework, we calculate the expected interaction rates for different scattering processes, including elastic and inelastic scattering off atomic electron shells, as well as loop-induced scattering off atomic nuclei. In those cases where the last effect dominates, leptophilic Dark Matter cannot be distinguished from conventional WIMPs. On the other hand, if inelastic scattering off the electron shell dominates, the expected event spectrum in direct detection experiments is different and would provide a distinct signal. However, we find that the signals in DAMA and/or CoGeNT cannot be explained by invoking leptophilic DM because the predicted and observed energy spectra do not match, and because of neutrino bounds from the Sun.

Identification of Dark Matter 2010
July 26 - 30 2010
University of Montpellier 2, Montpellier, France

*Speaker.

© Copyright owned by the author(s) under the terms of the Creative Commons Attribution-NonCommercial-ShareAlike Licence.

1. Introduction

The possibility that Dark Matter interacts predominantly with leptons has recently received a lot of attention [1 – 11], in particular in the context of cosmic ray anomalies [12 – 14] which could be due to Dark Matter annihilation. The phenomenology of leptophilic Dark Matter in direct detection experiments [15, 1, 16, 17] is somewhat less well explored, even though it has been noted [15] that a scattering process in which the recoil energy is transferred to electrons could explain the annual modulation signal observed in DAMA [18, 19] while remaining consistent with constraints from other experiments which treat electron recoils as background. For similar reasons, one might also hope to explain the CoGeNT signal [20] by invoking leptophilic Dark Matter.

In this talk, which is mainly based on Ref. [17], we study in detail the expected direct detection signals from leptophilic Dark Matter scattering. We will introduce our formalism, based on an effective field theory description of Dark Matter scattering, in sec. 2, and then proceed to a discussion of the four different classes of processes that can occur when a leptophilic weakly interacting massive particle (WIMP) interacts in a detector: WIMP-electron scattering, elastic and inelastic WIMP-atom scattering, and loop-induced WIMP-nucleus scattering. In sec. 3, we present exclusion limits on leptophilic Dark Matter from various direct detection experiment, and in sec. 4 we supplement these results with limits on leptophilic WIMP annihilation into neutrinos in the Sun. We summarize our results and conclude in sec. 5.

2. Leptophilic Dark Matter

Interactions between a Dark Matter (DM) fermion χ and charged leptons ℓ can be introduced in a model-independent way by considering the effective operator

$$\mathscr{L}_{\text{eff}} = \sum_i G\,(\bar{\chi}\Gamma^i_\chi \chi)\,(\bar{\ell}\Gamma^i_\ell \ell) \qquad \text{with} \qquad G = \frac{1}{\Lambda^2}\,, \tag{2.1}$$

where Λ is the UV-completion scale of the effective field theory, and Γ_χ, Γ_ℓ are Lorentz tensors. In principle, one can consider the following Lorentz structures:

$$\begin{aligned}
&\text{scalar (S) / pseudoscalar (P):} && \Gamma_\chi = c^\chi_S + i c^\chi_P \gamma_5, && \Gamma_\ell = c^\ell_S + i c^\ell_P \gamma_5\,,\\
&\text{vector (V) / axial vector (A):} && \Gamma^\mu_\chi = (c^\chi_V + c^\chi_A \gamma_5)\gamma^\mu, && \Gamma_{\ell\mu} = (c^\ell_V + c^\ell_A \gamma_5)\gamma_\mu\,,\\
&\text{tensor (T) / axial tensor (AT):} && \Gamma^{\mu\nu}_\chi = (c_T + i c_{AT}\gamma_5)\sigma^{\mu\nu}, && \Gamma_{\ell\mu\nu} = \sigma_{\mu\nu}\,.
\end{aligned} \tag{2.2}$$

However, it is straightforward to show [17] that for many of these operators, the low-energy WIMP-electron scattering cross section is proportional to v^2, where v is the WIMP velocity. Since, in units of the speed of light, $v^2 \sim \mathscr{O}(10^{-6})$, these terms are negligible in direct detection experiments unless all unsuppressed terms are absent and the cutoff scale Λ is very low. While this possibility cannot be excluded in a model-independent way, it is ruled out in many concrete DM models, which is why in most studies only the unsuppressed operators

$$\begin{aligned}
&S\otimes S: && G\,(\bar{\chi}\chi)\,(\bar{\ell}\ell)\,, && V\otimes V: && G\,(\bar{\chi}\gamma^\mu\chi)\,(\bar{\ell}\gamma_\mu\ell)\,,\\
&A\otimes A: && G\,(\bar{\chi}\gamma^\mu\gamma^5\chi)\,(\bar{\ell}\gamma_\mu\gamma^5\ell)\,, && T\otimes T: && G\,(\bar{\chi}\sigma^{\mu\nu}\chi)\,(\bar{\ell}\sigma_{\mu\nu}\ell)
\end{aligned} \tag{2.3}$$

are considered. Here, we will in particular focus on $V \otimes V$ and $A \otimes A$ operators since we will see that, as far as the direct detection phenomenology is concerned, operators with other Lorentz structures are qualitatively similar to either of the two.

A leptophilic WIMP can interact in a detector in four different ways:

(i) WIMP-electron scattering. If the WIMP interacts with a weakly bound electron (i.e. the energy transferred to the electron is much larger than its binding energy to the atomic nucleus), the electron will be kicked out of the atom to which it is bound, while the atom remains at rest. The typical electron recoil energy in processes of this type if of order $m_e v^2 \lesssim 1$ eV, far below the $\mathscr{O}(\text{keV})$ detection thresholds of DM direct detection experiments. However, since the electron is initially in a bound state, there is a small probability that it enters the interaction with a very high initial state momentum. In this case the kinematics is different, and $\mathscr{O}(\text{keV})$ recoil energies are possible, though unlikely. More precisely, the differential event rate for axial-vector WIMP-electron scattering is given by

$$\frac{dR}{dE_d} \simeq \frac{3\rho_0 m_e G^2}{4\pi m_\text{A} m_\chi} \sum_{nl} \sqrt{2m_e(E_d - E_{B,nl})}\,(2l+1) \int \frac{dp\,p}{(2\pi)^3}\,|\chi_{nl}(p)|^2 I(v_\text{min})\,, \tag{2.4}$$

where m_χ is the WIMP mass, $\rho_0 \sim 0.3$ GeV cm^{-3} is the local DM density m_A is the mass of the target atom, E_d is the observed electron recoil energy, $E_{B,nl}$ is the binding energy of the (n,l) atomic shell, and $\chi_{nl}(p)$ is the radial part of the momentum-space wave function of that shell, normalized according to $\int dp\,(2\pi)^{-3} p^2 |\chi_{nl}(p)|^2 = 1$. The function $I(v_\text{min})$ is defined by $I(v_\text{min}) \equiv \int d^3v\;\; v^{-1} f(\mathbf{v})\,\theta(v - v_\text{min})$, with the WIMP velocity distribution $f(\mathbf{v})$ and the minimum WIMP velocity required to obtain a recoil energy E_d given by $v_\text{min} \approx E_d/p + p/2m_\chi$. To arrive at eq. (2.4), we have evaluated the Feynman diagram of WIMP-electron scattering, taking into account the modified kinematics for bound systems, and replacing the usual plane wave initial states with the appropriate bound state wave functions. Comparing eq. (2.4) to the rate for conventional WIMP-nucleus scattering through axial-vector couplings in a nucleophilic model,

$$\frac{dR^0}{dE_d} \simeq \frac{3\rho_0 G^2}{2\pi m_\chi} I(v^0_\text{min}) \qquad \text{with} \qquad v^0_\text{min} = \frac{m_\chi + m_N}{m_\chi}\sqrt{\frac{E_d}{2m_N}}\,, \tag{2.5}$$

we find that (2.4) is suppressed compared to (2.5) by a factor of order $m_e/m_A \times \sqrt{2m_e E_d}\,p^2|\chi_{nl}(p)|^2$. For $m_\chi \gtrsim 10$ GeV, the relevant values for p (i.e. those which lead to the smallest possible v_min and hence to the largest possible value of $I(v_\text{min})$) are $p \sim \sqrt{2m_\chi E_d} \gtrsim 10$ MeV/c. In fig. 1, we plot $p^2|\chi_{nl}(p)|^2$ (which is proportional to the momentum distribution of the electron) as a function of p. We observe that $p^2|\chi_{nl}(p)|^2$ is extremely small in the relevant momentum region, so that dR/dE_d is hugely suppressed compared to dR^0/dE_d for similar values of G^2.

(ii) Elastic WIMP-atom scattering. If a WIMP interacts with one of the strongly bound inner electrons of one of the target atoms, the energy transfer is not sufficient to overcome the electron binding energy, and the recoil will be taken up by the atom as a whole. Experimentally, such events would resemble conventional nuclear recoils. However, it turns out that elastic WIMP-atom scattering is always subdominant compared to other processes [17], so we will not consider it further here.

(iii) Inelastic WIMP-atom scattering. For scattering processes in which the energy transfer is comparable to the binding energy of the target electron, the electron may be excited to a less

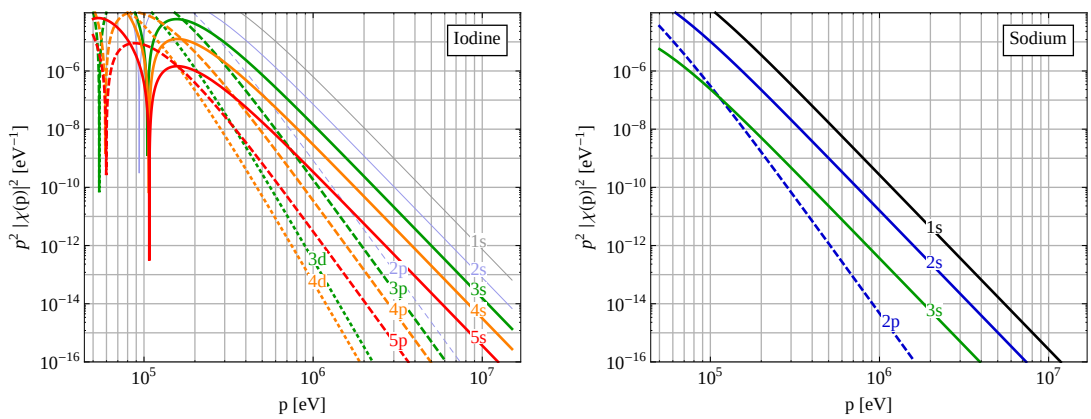

Figure 1: The momentum space electron wave functions of iodine and sodium. Thick colored curves correspond to shells that contribute to WIMP-electron scattering in DAMA, while thin light curves correspond to electrons that are too tightly bound to be separated from the atom in a WIMP interaction at DAMA energies. The approximate wave functions shown here are taken from ref. [21]. They do not include relativistic corrections (which can lead to flattening at high momentum) or multi-electron correlations.

strongly bound state, but still remain bound to the nucleus. In that case, as for elastic WIMP-atom scattering, the recoil momentum will be taken up by the atom as a whole. The event rate for inelastic WIMP-atom scattering is proportional to

$$\sum_{n'l'm'}\sum_{nlm}|\langle n'l'm'|e^{i(\mathbf{k}-\mathbf{k}')\mathbf{x}}|nlm\rangle|^2\,, \tag{2.6}$$

where (n,l,m) and (n',l',m') are the initial and final state quantum numbers of the electron and $\mathbf{k}$, $\mathbf{k}'$ are the initial and final WIMP momenta. Since the electron wave functions are tiny at the large momenta required in direct detection experiments, these matrix elements are tiny. Numerically, it turns out that inelastic WIMP-atom scattering is subdominant compared to WIMP-electron scattering [17]. However, in experiments that reject pure electron recoils as background, it may be the dominant contribution to the signal since it resembles WIMP-nucleus scattering.

(iv) Loop-induced WIMP-nucleus scattering. Even though tree level WIMP-nucleus scattering is forbidden in our leptophilic scenario, it may be induced at the loop level through the diagrams shown in fig. 2. While these diagrams are suppressed by one (1-loop) or two (2-loop) powers of αZ, multiplied by a loop factor, compared to tree-level WIMP-nucleus scattering in conventional nucleophilic DM models, the suppression is much less severe than that of WIMP-electron scattering *(i)* and WIMP-atom scattering *(ii)*, *(iii)*. This leads to the conclusion that, *whenever WIMP-nucleus scattering is possible, be it only at the loop-level, it will be the dominant process in direct detection experiments.* This in particular means that leptophilic DM can only reconcile the DAMA and CoGeNT signals with the null observations from other experiments if the loop-diagrams from fig. 2 vanish. This is, for example, the case for $A\otimes A$ couplings between DM and electrons.

We summarize this section with a rough numerical estimate for the relative rates of WIMP-atom scattering *(i)*, *(ii)* (WAS), WIMP-electron scattering *(iii)* (WES), and loop-induced WIMP-nucleus scattering *(iv)* (WNS) [17]:

$$R^{\text{WAS}} : R^{\text{WES}} : R^{\text{WNS}} \sim\sim 10^{-17} : 10^{-10} : 1\,. \tag{2.7}$$

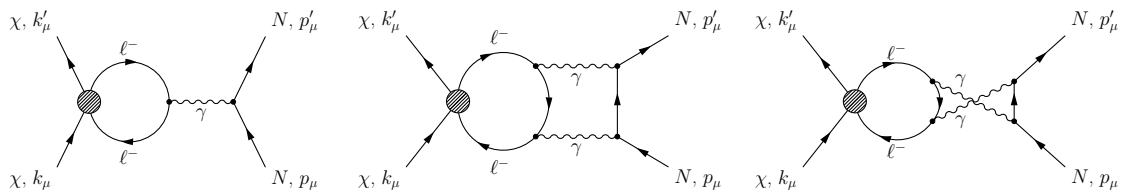

Figure 2: DM-nucleus interaction induced by a charged lepton loop and photon exchange.

3. Exclusion limits on leptophilic Dark Matter from direct detection experiments

Let us now consider experimental constraints on leptophilic DM from direct detection experiments. In fig. 3, we show constraints on the WIMP mass and the WIMP–free electron cross section σ_e^0 derived from CDMS [22], XENON-10 [23], CoGeNT [20], and DAMA [18] data. We also compare the DAMA annual modulation spectrum to the signal predicted for leptophilic DM. We see that for $V \otimes V$ interactions, the spectral fit to the DAMA data is good, but the tension between DAMA/CoGeNT and CDMS/XENON-10 is the same as in non-leptophilic models. This is easily understandable because in the $V \otimes V$ case, the loop diagrams fig. 2 are non-zero, so the dominant signal in all experiments is due to WIMP-nucleus scattering. On the other hand, for $A \otimes A$ interactions, WIMP-nucleus scattering is absent, so only the much weaker inelastic WIMP-atom scattering contributes to the CDMS/XENON-10 exclusion limits, while the DAMA/CoGeNT signals are explained by the less-suppressed WIMP-electron scattering. Note that the analysis of electron background events in CDMS, ref. [24], could be used to improve the CDMS limit, even though it would still be consistent with the DAMA/CoGeNT-favored parameter region. A careful analysis of the extremely low electron background in XENON-100 [25], however, may rule out that region. In any case, the fit to the DAMA modulation spectrum (and the fit to the spectrum of excess events in CoGeNT) is very poor in the case of $A \otimes A$ couplings because the steep decrease of the electron wave functions at high momentum (fig. 1) leads to a too steeply decreasing modulation spectrum. This rules out leptophilic DM with $A \otimes A$ couplings as an explanation for the DAMA and/or CoGeNT signals. Since, as far as direct detection experiments are concerned, $V \otimes V$ and $A \otimes A$ interactions encompass all phenomenologically different types of leptophilic DM models, we conclude that leptophilic DM cannot reconcile DAMA and CoGeNT with other experiments.

4. Neutrinos from Dark Matter annihilation in the Sun

In addition to constraints from direct detection experiments, we have also considered DM capture and annihilation in the Sun, which may lead to detectable neutrino signals. Since scattering on the free electrons in the Sun is sufficient for a WIMP to be captured, DM capture in the Sun does not receive the same suppression as WIMP-electron scattering observable in direct detection experiments. Still, in those cases where WIMP-nucleus scattering is allowed, it is the dominant capture reaction. For direct detection, it was sufficient to assume DM couplings to electrons (which would not lead to annihilation of the captured WIMPs into neutrinos), but it is very natural to assume that interactions with electrons are accompanied by interactions with other leptons. Even without that additional assumption, annihilation into neutrinos can be induced by loop diagrams similar to those shown in fig. 2, by a diagram in which two DM particles annihilate into virtual

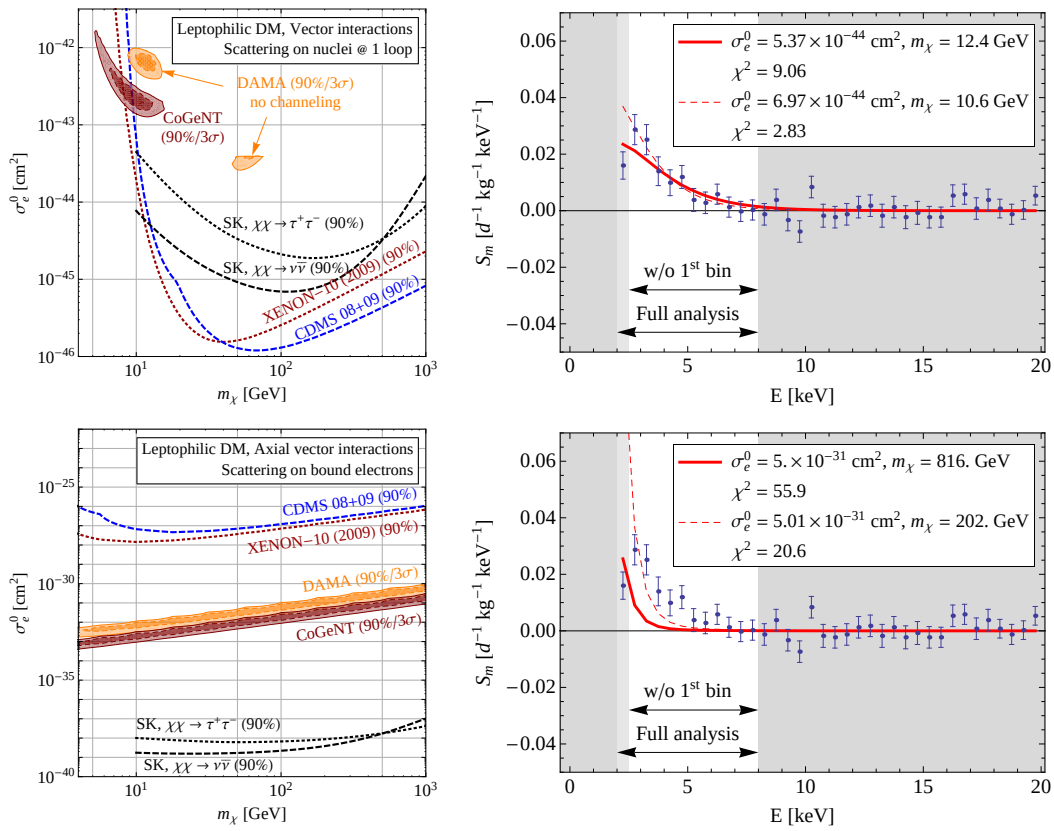

Figure 3: Left: CDMS, XENON-10, and Super-Kamiokande exclusion limits and DAMA/CoGeNT-favored values for the WIMP mass m_χ and the WIMP–fre electron scattering cross section σ_e^0. Right: comparison of the observed annual modulation spectrum in DAMA to the prediction for leptophilic DM. The solid curve has been fitted to the DAMA data from 2–8 keV, while for the dashed curve, the first energy bin has been neglected. The top row of panels is for $V \otimes V$ interactions, while the bottom row is for $A \otimes A$ interactions.

electrons which then exchange a W boson and turn into neutrinos, or by W/Z radiation [26]. On the other hand, neutrino signals from DM annihilation can be absent if there exists a particle-antiparticle asymmetry in the DM sector. If we neglect this possibility, we can derive constraints on leptophilic DM from Super-Kamiokande data [27] (black curves in fig. 3). These constraints are comparable to direct detection constraints when WIMP-nucleus scattering dominates, but much stronger than direct detection constraints when WIMP-electron scattering is most important. Thus, even though Super-Kamiokande limits are not as model-independent as direct detection constraints, they strongly support our conclusion that leptophilic DM cannot explain the DAMA signal.

5. Conclusions

In conclusion, we have studied the phenomenology of the well-motivated leptophilic Dark Matter scenario in direct detection experiments and have made detailed predictions for the observable signals. In particular, we have classified leptophilic DM interactions into elastic WIMP-atom scattering, inelastic WIMP-atom scattering, WIMP-electron scattering, and loop-induced WIMP-nucleus scattering, with the first one having the smallest cross section and the last one the largest, unless the relevant loop-diagrams are forbidden by symmetry arguments. We have then computed

model-independent constraints on the parameter space of leptophilic DM from CDMS, XENON-10, CoGeNT, and DAMA data, and slightly model-dependent constraints from Super-Kamiokande data on DM-induced neutrino signals from the Sun. While our study shows that leptophilic DM has a rich and interesting phenomenology, we have also seen that it cannot explain the DAMA/CoGeNT signals while remaining consistent with null results from other experiments.

Acknowledgments

It is a pleasure to thank Marco Cirelli, Nicolao Fornengo, Roni Harnik, Alexander Merle, Thomas E. J. Underwood, and Andreas Weiler for very useful discussions, and the organizers of the IDM 2010 conference for a very enjoyable and productive meeting. This work was in part supported by the Sonderforschungsbereich TR 27 of the Deutsche Forschungsgemeinschaft. JK received support from the Studienstiftung des Deutschen Volkes. Fermilab is operated by Fermi Research Alliance, LLC under Contract No. DE-AC02-07CH11359 with the US DOE.

References

[1] P. J. Fox and E. Poppitz, Phys. Rev. **D79** (2009), 083528, [arXiv:0811.0399].
[2] A. Ibarra, A. Ringwald, D. Tran, and C. Weniger, JCAP **0908** (2009), 017, [arXiv:0903.3625].
[3] D. Spolyar, M. Buckley, K. Freese, D. Hooper, and H. Murayama, (2009), [arXiv:0905.4764].
[4] E. J. Chun, J.-C. Park, and S. Scopel, JCAP **1002** (2010), 015, [arXiv:0911.5273].
[5] B. Kyae, JCAP **0907** (2009), 028, [arXiv:0902.0071].
[6] X.-J. Bi, X.-G. He, and Q. Yuan, Phys.Lett. **B678** (2009), 168–173, [arXiv:0903.0122].
[7] H. Davoudiasl, Phys.Rev. **D80** (2009), 043502, [arXiv:0904.3103].
[8] T. Cohen and K. M. Zurek, Phys.Rev.Lett. **104** (2010), 101301, [arXiv:0909.2035].
[9] Y. Farzan, S. Pascoli, and M. A. Schmidt, (2010), [arXiv:1005.5323].
[10] N. Haba, Y. Kajiyama, S. Matsumoto, H. Okada, and K. Yoshioka, (2010), [arXiv:1008.4777].
[11] A. E. Erkoca, M. H. Reno, and I. Sarcevic, (2010), [arXiv:1009.2068].
[12] PAMELA, O. Adriani et al., Nature **458** (2009), 607–609, [arXiv:0810.4995].
[13] The Fermi LAT, A. A. Abdo et al., Phys. Rev. Lett. **102** (2009), 181101, [arXiv:0905.0025].
[14] D. Hooper and L. Goodenough, (2010), [arXiv:arXiv:1010.2752], * Temporary entry *.
[15] R. Bernabei et al., Phys. Rev. **D77** (2008), 023506, [arXiv:0712.0562].
[16] A. Dedes, I. Giomataris, K. Suxho, and J. D. Vergados, (2009), [arXiv:0907.0758].
[17] J. Kopp, V. Niro, T. Schwetz, and J. Zupan, Phys. Rev. **D80** (2009), 083502, [arXiv:0907.3159].
[18] DAMA, R. Bernabei et al., Eur. Phys. J. **C56** (2008), 333–355, [arXiv:0804.2741].
[19] R. Bernabei et al., Eur.Phys.J. **C67** (2010), 39–49, [arXiv:1002.1028].
[20] CoGeNT, C. E. Aalseth et al., (2010), [arXiv:1002.4703].
[21] C. F. Bunge, J. A. Barrientos, and A. V. Bunge, At. Data Nucl. Data Tables **53** (1993), 113 – 162.
[22] CDMS, Z. Ahmed et al., Phys. Rev. Lett. **102** (2009), 011301, [arXiv:0802.3530].
[23] XENON, J. Angle et al., Phys. Rev. Lett. **100** (2008), 021303, [arXiv:0706.0039].
[24] CDMS Collaboration, Z. Ahmed et al., Phys.Rev. **D81** (2010), 042002, [arXiv:0907.1438].
[25] XENON100 Collaboration, E. Aprile et al., Phys.Rev.Lett. **105** (2010), 131302, [arXiv:1005.0380].
[26] N. F. Bell, J. B. Dent, T. D. Jacques, and T. J. Weiler, (2010), [arXiv:1009.2584].
[27] Super-Kamiokande, S. Desai et al., Phys. Rev. **D70** (2004), 083523, [arXiv:hep-ex/0404025].